



Brain Cancer Cell Classification Method Using Computed Aided Diagnosis (CAD) System

Hmmam T.Hassan,M.Sc, Zeinab A.Mustafa,PhD, Banazier A.Ibraheem,PhD & Rania.E Mahdi,PhD.

Abstract

Automatic classification of the brain tumor may increase the efficiency and save the time for diagnosing brain tumor; early detection of brain cancer can increase the chance of survival among people. Computed aided diagnosis system for the classification of brain cancer is developed. Overall, there are three main processes used throughout the report; data collection, image processing and finally the classification process. MATLAB is used in every process made throughout the project. Computer aided diagnosis (CAD) systems can enhance the diagnostic capabilities of physicians and reduce the time required for accurate diagnosis. The experiments were carried out on 50 images consisting of 20 normal and 50 abnormal (malignant and benign tumors) from a real human brain MRI dataset. Haralick's texture features extracted from the ROI the effective features are then classified using feed-forward back propagation neural network. The classification accuracy is 96% which was significantly good. Moreover, the proposed technique demonstrates its effectiveness compared with the other machine learning recently published techniques. The results revealed that the proposed hybrid approach is accurate and fast and robust. Finally, possible future directions are suggested.

Keywords: Brain tumor, Computed Aided diagnosis, Haralick's texture features, neural network.

i. Introduction

Cancer of the brain is usually called a brain tumor. When most normal cells grow old or get damaged, they die, and new cells take their place. Sometimes, this process goes wrong. New cells form when the body doesn't need them, and old or damaged cells don't die as they should. The buildup of extra cells often forms a mass of tissue called a growth or tumor [1] [2]. Primary brain tumors can be benign or malignant:

Benign: brain tumors do not contain cancer cells, usually, benign tumors can be removed, and they Seldom grow back; benign brain tumors usually have an obvious border or edge. Cells from benign tumors rarely invade tissues around them. They don't spread to other parts of the body. However, benign tumors can press on sensitive areas of the brain and cause serious health problems, unlike benign tumors in most other parts of the body, benign brain tumors are sometimes life threatening, benign brain tumors may become malignant [2].

Malignant: brain tumors (also called brain cancer) contain cancer cells malignant brain tumors are generally more serious and often are a threat to life, they are likely to grow rapidly

Cite this article as: Hmmam T.Hassan, Zeinab A.Mustafa, Banazier A.Ibraheem & Rania.E Mahdi, " Brain Cancer Cell Classification Method Using Computed Aided Diagnosis (CAD) System", International Journal of Research in Advanced Computer Science Engineering, (IJRACSE), Volume



and crowd or invade the nearby healthy brain tissue, Cancer cells may break away from malignant brain tumors and spread to other parts of the brain or to the spinal cord. They rarely spread to other parts of the body [2].

The symptoms of a brain tumor depend on tumor size, type, and location. Symptoms may be caused when a tumor presses on a nerve or harms a part of the brain. Also, they may be caused when a tumor blocks the fluid that flows through and around the brain, or when the brain swells because of the buildup of fluid [2].

ii. Methodology

a. Data collection

All MRI scan images of brain that used on this project were collected from Harvard citations from were found in the Web of Science database. The entire MRI scan is in GIF format .The database consists of 20 images of normal brain from a women in a range of (51 - 81) years old, in excellent health, who participated in research on normal aging, and 30 images with brain tumor from A women sought medical attention because of gradually increasing right hemiparesis (weakness) and hemianopia (visual loss). At craniotomy (8/90), left parietal anaplastic astrocytoma was found. A right frontal lesion was biopsied in (8/94). Recurrent tumor was suspected on the basis of the imaging, and was confirmed pathologically [3].

b. Image processing

Image processing procedures play the most crucial part for the project. The original images in the Gif format, the first step is transfer the images into JBEG format, and then the bilateral filter is used.

The region of interest on the image is area of tumor which is needed to extract the features from it. To select this area, the function IMCROP on MATLAB is used, the area of the tumor is precisely selected.

c. Features Extraction

Feature extracted using SGLDM from the region of interest then it tested using ttest function to be used for next step.

d. Feature classification

There are a large number of statistical learning methods that can be applied to this image classification problem. In this project the feed-forward back propagation neural network was used.

Artificial neural networks are biologically inspired classification algorithms that consist of an input layer of nodes, one or more hidden layers and an output layer. Each node in a layer has one corresponding node in the next layer, thus creating the stacking effect [4]. Artificial neural networks are the very versatile tools and have been widely used to tackle many issues [5, 6]. Feed-forward neural networks (FNN) are one of the popular structures among artificial neural networks. These efficient networks are widely used to solve complex problems by modeling complex input-output relationships [7, 8].

BPLAs were proposed by Rumelhart et al. [9]. They have since become famous learning algorithms among ANNs. In the learning process, to reduce the inaccuracy of ANNs, BPLAs use the gradient-descent search method to adjust the connection weights. The structure of a back-propagation ANN is shown in Figure below. The output of each neuron is the aggregation of the numbers of neurons of the previous level multiplied by its corresponding weights. The input values are converted into output signals with the calculations of activation functions [10]. Back-propagation ANNs have been widely and successfully applied in diverse applications, such as pattern recognition, location selection and performance evaluations.

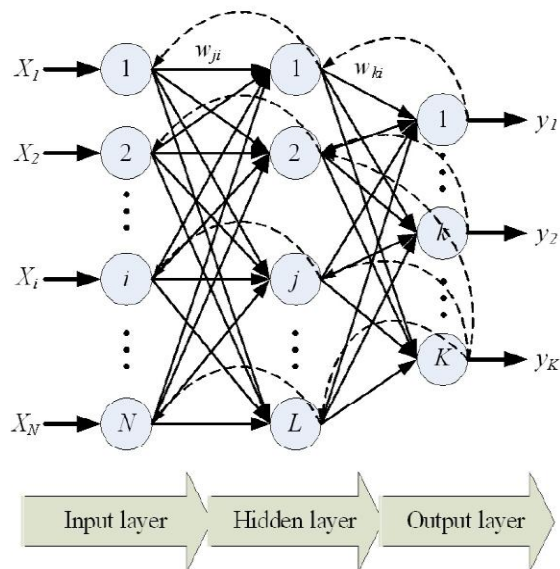


Figure 1: Back-propagation ANN

iii. Results and Discussion

The two images below shows the differences of the filtered image from the original image, when applying the bilateral filtering.



Figure 2: Original Image

Figure 3: Filtered image

The differences are very clear on the filtered image it's appearing more sharp with more details and with less noise. The next step is to take the region of interest from the filtered image.

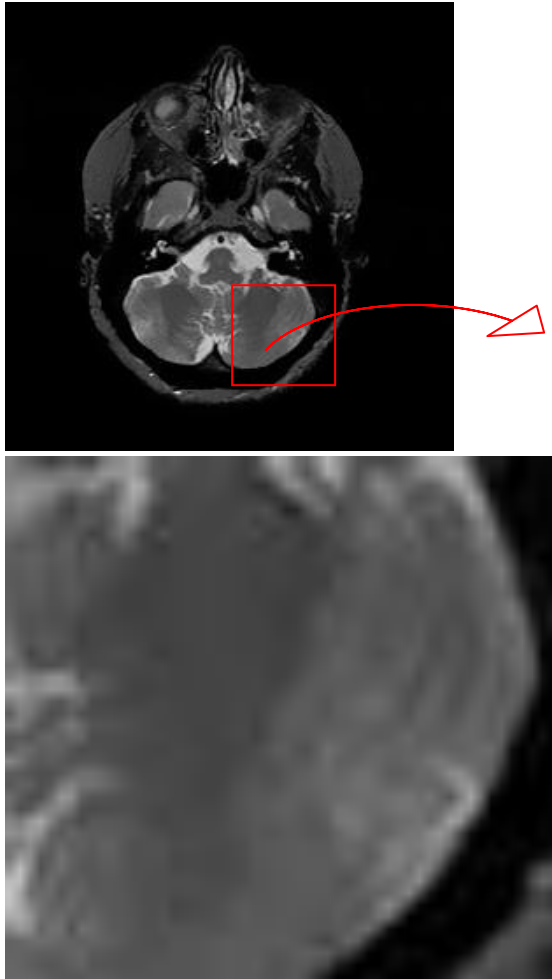


Figure 4: Selection of the region of interest (ROI)

The region of interest which contains the tumor tissue in the cancerous images was selected to be used for the next step.

Feature extraction was done one the selected region using spatial gray level dependence matrices (SGLDM) method, the (SGLDM) returns two values mf and rf as shown in the two figures below.

Type	Energy	Contrast	Correlation	Variance	Homogeneity	Sum average	Sum variance	Sum entropy	Entropy	Diff variance	Diff entropy	Diff average	Measures of correlation
T	0.0000	0.2916	0.0008	0.8127	0.0002	0.1738	2.9591	0.0049	0.0068	0.2100	0.0031	-0.0004	0.0010
T	0.0000	0.3162	0.0009	1.2730	0.0003	0.1543	4.7758	0.0051	0.007	0.2446	0.0030	-0.0004	0.0010
T	0.0000	0.4513	0.0009	2.2535	0.0003	0.1446	8.3705	0.0052	0.0069	0.3470	0.0031	-0.0005	0.0010
T	0.0000	0.3180	0.0009	2.0471	0.0002	0.1561	7.8602	0.0054	0.0073	0.2205	0.0033	-0.0004	0.0010
T	0.0000	0.2941	0.0009	1.4785	0.0002	0.1742	5.6198	0.0049	0.0071	0.1937	0.0033	-0.0003	0.0010
T	0.0000	0.3599	0.0009	1.7637	0.0002	0.1899	4.6909	0.0050	0.0073	0.2295	0.0034	-0.0003	0.0010
T	0.0000	0.3767	0.0009	1.8885	0.0002	0.1925	4.7773	0.0051	0.0075	0.2339	0.0035	-0.0003	0.0010
T	0.0000	0.3948	0.0008	1.3146	0.0002	0.1888	4.8637	0.0050	0.0073	0.2573	0.0034	-0.0004	0.0010
T	0.0000	0.3736	0.0009	1.5399	0.0002	0.1653	5.7860	0.0051	0.0072	0.2532	0.0033	-0.0004	0.0010
T	0.0000	0.4172	0.0008	1.3096	0.0002	0.1789	4.8210	0.0052	0.0074	0.2733	0.0034	-0.0004	0.0010
T	0.0000	0.4561	0.0009	1.6188	0.0002	0.1778	6.0190	0.0052	0.0073	0.2968	0.0034	-0.0004	0.0010
T	0.0000	0.3946	0.0009	2.3828	0.0002	0.2412	8.7365	0.0055	0.0077	0.2461	0.0034	-0.0004	0.0010
T	0.0000	0.4234	0.0009	2.4997	0.0002	0.2811	9.5762	0.0055	0.0077	0.2597	0.0035	-0.0004	0.0010
T	0.0000	0.0395	0.0001	0.3204	0.0000	0.0282	1.2421	0.0006	0.0007	0.0251	0.0003	0.0000	0.0010
T	0.0000	0.0553	0.0001	0.2788	0.0000	0.0304	1.0599	0.0006	0.0008	0.0342	0.0004	0.0000	0.0010
T	0.0000	0.0553	0.0001	0.2900	0.0000	0.0322	1.1048	0.0006	0.0008	0.0351	0.0004	0.0000	0.0010
T	0.0000	0.5231	0.0009	2.2998	0.0002	0.3596	8.6761	0.0055	0.0076	0.3091	0.0036	-0.0005	0.0010
T	0.0000	0.4973	0.0009	2.0825	0.0002	0.3718	7.8327	0.0055	0.0075	0.3031	0.0036	-0.0005	0.0010
T	0.0000	0.7121	0.0009	2.5230	0.0001	0.3697	9.3801	0.0056	0.0079	0.4263	0.0038	-0.0004	0.0010
T	0.0000	0.0679	0.0001	0.2675	0.0000	0.0373	1.0020	0.0006	0.0008	0.0390	0.0004	0.0000	0.0010
T	0.0000	0.0640	0.0001	0.2843	0.0000	0.0360	1.0732	0.0006	0.0008	0.0357	0.0004	0.0000	0.0010
T	0.0000	0.6779	0.0008	1.9836	0.0001	0.3493	7.2564	0.0057	0.0079	0.3467	0.0039	-0.0004	0.0010
T	0.0000	0.7270	0.0009	2.4412	0.0001	0.3401	9.0378	0.0057	0.0077	0.3858	0.0039	-0.0005	0.0010
T	0.0000	0.0835	0.0001	0.2795	0.0000	0.0356	1.0346	0.0006	0.0008	0.0451	0.0004	0.0000	0.0010
T	0.0000	0.7052	0.0008	1.8960	0.0001	0.3816	6.8790	0.0055	0.0076	0.4004	0.0038	-0.0004	0.0010
T	0.0000	0.7240	0.0008	2.4011	0.0001	0.3991	8.8804	0.0054	0.0075	0.4447	0.0037	-0.0004	0.0010
T	0.0000	0.0928	0.0001	0.5377	0.0000	0.0355	2.0582	0.0006	0.0008	0.0558	0.0004	0.0000	0.0010
T	0.0000	0.0967	0.0001	0.5389	0.0000	0.0346	2.0590	0.0006	0.0008	0.0553	0.0004	0.0000	0.0010
T	0.0000	0.1121	0.0001	0.6324	0.0000	0.0306	2.4174	0.0006	0.0008	0.0622	0.0004	0.0000	0.0010
T	0.0000	0.0967	0.0001	0.5080	0.0000	0.0341	1.9331	0.0006	0.0007	0.0602	0.0004	-0.0001	0.0010
N	0.0000	0.1818	0.0008	0.3728	0.0003	0.1628	1.2095	0.0045	0.0064	0.1337	0.0028	-0.0003	0.0010
N	0.0000	0.4608	0.0007	0.9199	0.0002	0.1850	3.2188	0.0049	0.0071	0.3006	0.0034	-0.0003	0.0010
N	0.0000	0.7204	0.0008	1.8194	0.0001	0.2250	6.5573	0.0054	0.0078	0.4082	0.0038	-0.0004	0.0010
N	0.0000	0.5675	0.0008	1.4750	0.0002	0.1793	5.3325	0.0051	0.0070	0.4008	0.0033	-0.0004	0.0010
N	0.0000	0.3155	0.0009	1.2552	0.0002	0.1913	4.6553	0.0050	0.0071	0.2502	0.0032	-0.0004	0.0010
N	0.0000	0.3722	0.0008	1.3006	0.0002	0.1875	4.4302	0.0051	0.0071	0.2656	0.0032	-0.0004	0.0010
N	0.0000	0.4488	0.0009	1.7671	0.0002	0.1776	6.6195	0.0051	0.0070	0.3277	0.0032	-0.0004	0.0010
N	0.0000	0.4763	0.0009	1.7226	0.0002	0.2001	6.4141	0.0050	0.0069	0.3430	0.0032	-0.0004	0.0010
N	0.0000	0.4052	0.0009	1.4280	0.0002	0.1947	5.2067	0.0049	0.0069	0.2932	0.0032	-0.0004	0.0010
N	0.0000	0.3672	0.0008	1.2224	0.0002	0.1867	4.5225	0.0048	0.0068	0.2895	0.0031	-0.0004	0.0010
N	0.0000	0.4045	0.0009	1.5922	0.0002	0.2093	5.9645	0.0050	0.0071	0.2965	0.0031	-0.0004	0.0010
N	0.0000	0.2638	0.0009	0.8918	0.0003	0.1840	3.3033	0.0047	0.0064	0.2049	0.0028	-0.0004	0.0010
N	0.0000	0.3458	0.0008	0.8889	0.0003	0.1880	3.2100	0.0048	0.0067	0.2549	0.0030	-0.0004	0.0010
N	0.0000	0.3287	0.0009	1.1043	0.0003	0.1949	4.0886	0.0048	0.0067	0.2369	0.0031	-0.0004	0.0010
N	0.0000	0.5342	0.0008	1.7026	0.0002	0.2193	6.2760	0.0052	0.0072	0.3614	0.0034	-0.0004	0.0010
N	0.0000	0.4121	0.0008	1.1870	0.0002	0.1975	4.3359	0.0049	0.0069	0.2784	0.0033	-0.0004	0.0010
N	0.0000	0.5315	0.0008	1.3459	0.0002	0.2113	4.8520	0.0051	0.0071	0.3653	0.0033	-0.0004	0.0010
N	0.0000	0.6059	0.0008	1.5312	0.0002	0.2076	5.5189	0.0051	0.0071	0.4163	0.0034	-0.0004	0.0010
N	0.0000	0.8789	0.0008	2.3182	0.0002	0.2091	8.3941	0.0055	0.0075	0.5654	0.0036	-0.0004	0.0010
N	0.0000	0.7262	0.0008	1.7599	0.0002	0.2037	6.3133	0.0050	0.0071	0.5251	0.0033	-0.0004	0.0010

(a)

Type	Energy	Contrast	Covariance	Variance	Homogeneity	Sum average	Sum variance	Sum entropy	Entropy	Difference	Difference entropy	Difference average	Measures of correlation
T	0.0009	211.2714	0.0481	17.6831	0.0420	0.4569	282.1039	0.0293	0.1737	149.2670	0.2796	0.0392	0.0207
T	0.0006	223.2451	0.0914	41.6409	0.0608	0.7639	368.0007	0.0340	0.1900	183.4608	0.2480	0.0442	0.0247
T	0.0011	480.6291	0.1075	20.0290	0.0393	1.2095	560.7452	0.0523	0.1271	381.0471	0.2119	0.0277	0.0215
T	0.0014	204.7664	0.0802	24.6661	0.0653	1.2544	423.4307	0.0369	0.2266	236.5446	0.4126	0.0438	0.0200
T	0.0015	276.4248	0.0959	49.2573	0.0669	1.4284	474.4540	0.0118	0.2972	176.8614	0.4855	0.0698	0.0173
T	0.0004	266.7753	0.1588	62.8702	0.0380	1.3639	632.7730	0.0255	0.2182	252.6752	0.4955	0.0531	0.0234
T	0.0005	205.2218	0.1199	13.4797	0.0454	0.4264	353.4158	0.0442	0.1535	183.6709	0.2697	0.0247	0.0291
T	0.0009	341.1509	0.1306	27.4217	0.0529	0.3999	415.6057	0.0553	0.1991	212.2594	0.2656	0.0480	0.0109
T	0.0010	271.9839	0.1223	30.2148	0.0509	0.3488	491.2129	0.0889	0.1898	260.2555	0.2455	0.0437	0.0273
T	0.0005	38.8152	0.1486	25.3279	0.0572	0.2971	471.9511	0.0522	0.2113	242.1434	0.4240	0.0478	0.0284
T	0.0008	647.2456	0.2007	23.7352	0.0519	1.066	631.2602	0.0716	0.2369	441.7935	0.4717	0.0515	0.0205
T	0.0004	424.7729	0.0943	38.4343	0.0503	0.6206	572.2961	0.0279	0.1951	266.5621	0.5021	0.0407	0.0209
T	0.0003	262.9809	0.0729	40.1321	0.0505	1.9469	523.4293	0.0114	0.1519	218.9949	0.4122	0.0209	0.0205
T	0.0007	214.4136	0.0494	25.6124	0.0429	1.2707	398.4815	0.0219	0.1212	193.2249	0.2944	0.0269	0.0204
T	0.0001	404.2151	0.0740	45.4873	0.0402	1.4610	571.4669	0.0237	0.0907	247.6071	0.2486	0.0198	0.0212
T	0.0001	410.4783	0.0717	66.1948	0.0454	1.4429	648.9001	0.0275	0.0813	272.9085	0.2011	0.0184	0.0201
T	0.0001	257.6887	0.0796	50.6781	0.0424	0.8321	497.4116	0.0213	0.0657	213.9444	0.2112	0.0153	0.0209
T	0.0002	211.2956	0.0764	49.4277	0.0291	0.6785	445.7109	0.0211	0.0879	186.2207	0.2034	0.0204	0.0211
T	0.0001	446.2604	0.0939	184.6863	0.0276	2.6729	884.3470	0.0119	0.0940	261.2541	0.2973	0.0230	0.0209
T	0.0001	351.0894	0.1046	33.9191	0.0326	1.8976	678.2170	0.0154	0.2016	320.4856	0.2776	0.0243	0.0200
T	0.0001	403.2455	0.0716	46.1911	0.0312	0.6297	588.1100	0.0237	0.2052	217.2727	0.2159	0.0213	0.0203
T	0.0000	402.6109	0.1035	54.7200	0.0130	1.8938	621.5287	0.0405	0.0479	209.4844	0.2018	0.0110	0.0207
T	0.0000	354.9623	0.1147	16.7410	0.0272	1.2686	621.9263	0.0253	0.0425	311.1941	0.2071	0.0198	0.0204
T	0.0000	625.2491	0.1144	45.2391	0.0325	1.7609	796.1900	0.0309	0.0696	355.2580	0.2218	0.0145	0.0209
T	0.0001	488.5992	0.1874	71.9593	0.0279	1.2460	890.6234	0.0234	0.0940	442.6661	0.2416	0.0223	0.0216
T	0.0001	397.2957	0.1296	91.2428	0.0207	1.6432	928.9075	0.0511	0.0898	402.0804	0.2174	0.0217	0.0206
T	0.0004	655.6071	0.0800	72.0237	0.0288	1.5712	906.3476	0.0233	0.2063	432.2127	0.2153	0.0226	0.0215
T	0.0002	692.8810	0.0646	79.4969	0.0352	1.4421	996.8290	0.0060	0.1099	371.5259	0.2640	0.0226	0.0207
T	0.0005	816.2145	0.0917	43.0907	0.0239	1.5945	967.9519	0.0184	0.2047	428.2653	0.4025	0.0220	0.0211
T	0.0003	832.7669	0.0814	30.2472	0.0363	2.4566	940.2519	0.0409	0.2004	491.2723	0.4230	0.0183	0.0205
N	0.0007	119.0909	0.1642	14.8067	0.0518	0.1969	144.6257	0.0124	0.2630	91.8224	0.2699	0.0481	0.0145
N	0.0005	272.1153	0.1494	12.0600	0.0494	0.2108	302.2448	0.0387	0.1914	175.8437	0.2689	0.0449	0.0114
N	0.0002	496.0922	0.1252	11.8071	0.0320	0.5776	448.9638	0.0120	0.2672	272.2041	0.2865	0.0230	0.0248
N	0.0005	345.9705	0.1192	16.9293	0.0290	0.2732	407.2213	0.0273	0.1202	254.5979	0.2414	0.0297	0.0209
N	0.0005	281.0836	0.1138	15.4021	0.0514	0.2469	342.7721	0.0094	0.1889	193.2620	0.2202	0.0449	0.0272
N	0.0004	226.8084	0.0959	17.8742	0.0423	0.4673	284.9935	0.0135	0.1540	163.5207	0.2958	0.0253	0.0263
N	0.0005	272.4068	0.0771	10.1227	0.0594	0.8513	281.5179	0.0271	0.1961	214.8173	0.2022	0.0415	0.0246
N	0.0005	277.6218	0.0805	5.2766	0.0628	0.5157	274.1035	0.0129	0.1703	194.2947	0.2008	0.0423	0.0208
N	0.0004	209.9412	0.0745	11.4968	0.0463	0.2117	349.1275	0.0092	0.1121	155.9962	0.2270	0.0200	0.0251
N	0.0006	220.4239	0.0904	24.8895	0.0620	0.7099	298.0231	0.0270	0.1469	159.2232	0.2972	0.0414	0.0208
N	0.0005	259.2927	0.0808	9.4872	0.0446	0.1991	221.4480	0.0182	0.2023	187.2658	0.2071	0.0462	0.0284
N	0.0007	218.8452	0.1271	41.9883	0.0586	0.6177	348.2271	0.0197	0.2662	167.1262	0.2124	0.0416	0.0269
N	0.0004	235.4058	0.1293	34.4818	0.0548	0.6476	273.2231	0.0201	0.1527	177.6898	0.2974	0.0434	0.0289
N	0.0007	254.2024	0.1146	25.1029	0.0644	0.7598	267.2940	0.0225	0.1828	181.5995	0.2428	0.0478	0.0271
N	0.0004	452.5989	0.1229	41.1566	0.0573	0.2073	455.0912	0.0242	0.1925	292.6770	0.4525	0.0412	0.0253
N	0.0005	213.2671	0.1231	9.8615	0.0649	0.2017	343.2022	0.0259	0.1480	208.2773	0.2262	0.0270	0.0261
N	0.0005	421.2946	0.1581	14.4871	0.0553	0.6721	476.2108	0.0248	0.1974	268.2657	0.4494	0.0476	0.0261
N	0.0005	278.2579	0.1904	22.6593	0.0588	1.1154	624.7882	0.0211	0.1738	278.9950	0.4423	0.0430	0.0252
N	0.0003	278.2356	0.1690	15.1794	0.0694	0.4238	829.0523	0.0240	0.2096	446.9289	0.5095	0.0455	0.0237
N	0.0006	511.5236	0.1448	19.5479	0.0584	0.7175	477.6950	0.0167	0.1746	363.2029	0.2607	0.0297	0.0271

(b)

Figure 5: (a)The thirteen mf features of 30 brain tumor MRI images and 20 normal MRI images results from SGLDM (b) The thirteen

rf features of 30 brain tumor MRI images and 20 normal MRI images results from SGLDM

Each feature was tested using *ttest*. The mf features gives the significance only for the two features contrast and difference variance which is not enough features to be used for feature classification. The rf test gives better number of feature than mf, the significance features is variance, sum average, sum variance and sum entropy.

Those feature was used on the feed forward back propagation neural network, the result of the trained network is incredible it reach 96%.

Confusion matrix

The confusion matrix is a performance measure used to demonstrate the number of correct and incorrect predictions made by the classification model compared to the actual outcomes (target value) in the data.

The matrix encompasses the above stated parameters. Using the plot confusion function in MATLAB, the following values for the proposed classifier were obtained.

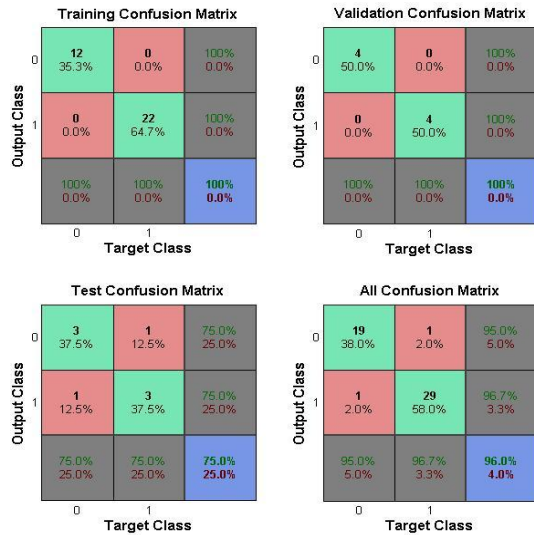


Figure 6: Confusion matrix

True Positives (TP)

Brain tissue marked as tumor tissues which were also classified as tumor tissue.

True Negatives (TN)

Brain tissues which were marked as Normal Brain tissue and that were also classified as Normal brain tissue.

False Positives (FP)

Tumor tissues which were marked as Normal tissue, but were classified as brain tumor tissue.

False Negatives (FN)

Tumor tissue which were marked as tumor tissue but which were classified as normal brain tissues.

The accuracy is the overall evaluation of the classifier for the pattern recognition and classification of the brain tumor. Therefore, the proposed system has successfully been

able to discriminate between tumor and normal tissue with a precision level of 96%.

Graphical User Interface (GUI)

The graphical user interface was designed for the system to be more applicable.

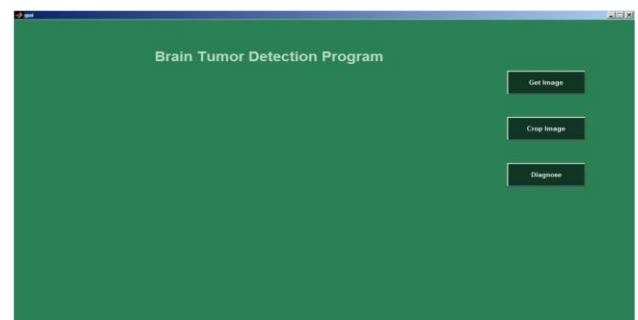


Figure 7: GUI for the brain tumor detection

The GUI contains three pushbutton named by get image, crop image and diagnose.

Get image: when it's pressed by the user it's automatically open the folder of the images to be selected by the user.

Crop image: it's used to select the region of interest (ROI) from the image.

Diagnose: when it's pressed its show the result of the diagnosing either its tumor tissue or normal tissue.

The two figures below shows two different diagnose by the system.



Figure 8: GUI of brain tumor diagnosis system with the illustration of a tumor tissue

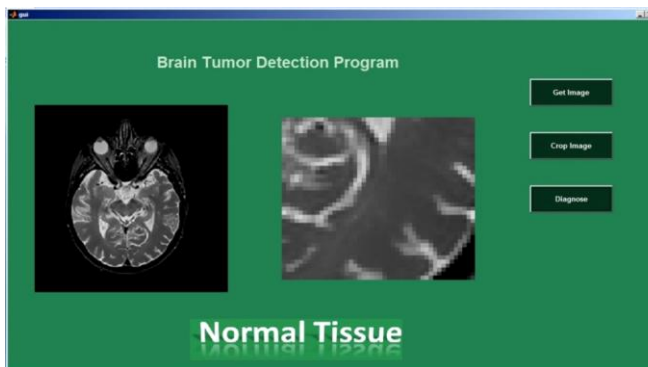


Figure 9: GUI of brain tumor diagnosis system with the illustration of a normal tissue

Conclusion

The algorithm were implemented based on 50 brain MRI images consisting of 20 normal and 30 abnormal (malignant and benign tumors) from a real human brain MRI dataset. The dataset used to performance evaluation. The dataset used consists of axial, T2-weighted, 256–256 pixel MR brain images. These images were collected from the Harvard Medical School website. A preprocessing stage should be considered to enhance the quality of the MRI brain before segmentation, feature extraction and classification. Image processing and enhancement stage is the simplest categories of medical image

processing. This stage is used for reducing image noise, highlighting edges, or displaying digital images. Applying the imcrop function on MATLAB for the segmentation of RIO in MRI image.

Based on adjusted and segmented images produced, a set of features are extracted from each image. Those features are tested using ttest function to select the significant features only. Back propagation feed forward neural network used to classify the selected feature. A graphical user interface (GUI) was designed to be easier for the use and to give better presentation.

iv. Conclusion and future work

With the advance of computational intelligence and machine learning techniques, computed aided diagnosis attracts more attention for brain tumor detection. It has become one of the most important research subjects in medical imaging and diagnostic radiology. In this study, we reviewed current studies of the different segmentation, feature extraction and classification algorithms. The proposed technique first employs the spatial gray level dependence matrices (SGLDM) to extract features from MRI images, and then applies feed forward back propagation neural network to classify inputs into normal or abnormal based on feature selection parameters. According to the experimental results, the designed method is efficient for automated diagnosis of brain tumor. The proposed method produces classification specificity of 92% rate. These experiment results show that the proposed classifier method can successfully differentiate between healthy and pathologically cases and can



increase the diagnostic performance of human brain abnormality. The challenge remains to provide a generalized CAD system that works in all cases regardless of database size and quality. So, CAD system remains an open problem. Future work would deal with classification of brain tumors into different grades by using advanced analysis methods, so that the surrender of brain tumor diagnosis can be increased. Using a large number of data from different sources.

References

- [1] Roberts T.A., Hyare H., Agliardi G., Hipwell B., d'Esposito A., Ianus A., Breen-Norris J.O., Ramasaw my R., Taylor V., Atkinson D., et al. Noninvasive diffusion magnetic resonance imaging of brain tumor cell size for the early detection of therapeutic response. *Sci. Rep.* 2020.
- [2] Biratu E.S., Schwenker F., Debelee T.G., Kebede S.R., Negera W.G., Molla H.T. Enhanced Region Growing for Brain Tumor MR Image Segmentation. *J. Imaging.* 2021;7:22.
- [3] Harvard medical school (2015). [Online]. Available: <http://www.med.harvard.edu/aanlib/home.htm> / .Geoscience and Remote Sensing, Vol. 33, No. 2, pp 293-304
- [4] S. Shrivastava and M. P. Singh, Performance evaluation of feed-forward neural network with soft computing techniques for hand written English alphabets, *Applied Soft Computing*, vol.11, no.1, pp.1156-1182, 2011.
- [5] Y. E. Shao and B.-S. Hsu, Determining the contributors for a multivariate SPC chart signal using artificial neural networks and support vector machine, *International Journal of Innovative Computing, Information and Control*, vol.5, no.12(B), pp.4899-4906, 2009.
- [6] D. K. Li, H. X. Zhang and S. A. Li, Development cost estimation of aircraft frame based on BP neural networks, *Fire Control and Command Control*, vol.31, no.9, pp.27-29, 2006.
- [7] B. Karimi, M. B. Menhaj and I. Saboori, Multilayer feed forward neural networks for controlling decentralized large-scale non-affine nonlinear systems with guaranteed stability, *International Journal of Innovative Computing, Information and Control*, vol.6, no.11, pp.4825-4841, 2010.
- [8] B. ZareNezhad and A. Aminian, A multi-layer feed forward neural network model for accurate prediction of ue gas sulfuric acid dew points in process industries, *Applied Thermal Engineering*, vol.30, no.6-7, pp.692696, 2010.
- [9] D. E. Rumelhart, G. E. Hinton and R. J. Williams, Learning representations by back-propagating errors, *Nature*, vol.323, no.6088, pp.533-536, 1986.
- [10] M. N. Hajmeer and I. A. Basheer, A hybrid bayesian-neural network approach for probabilistic modeling of bacterial growth/no-growth interface, *International Journal of Food Microbiology*, vol.82, no.3, pp.233243, 2003.

Author Details:



ISSN No : 2454-4221 (Print)
ISSN No : 2454-423X (Online)

International Journal of Research in Advanced Computer Science Engineering

A Peer Reviewed Open Access International Journal
www.ijracse.com

Hmmam T. Hassan, M.Sc. Department of Engineering, Faculty of Biomedical Engineering, University of Medical Sciences and Technology, Khartoum, Sudan, he can be reached at: hmmam_tahir@hotmail.com

Zeinab. A.Mustafa, PhD, is an Associate Professor in the Biomedical Engineering Department, College of Engineering, Sudan University of Sciences and Technology, East Diom, 61 St, P.O. Box 407, Khartoum, Sudan , she and can be reached at: zenab42000@yahoo.com

Banazier .A. Ibraheem, PhD, is an Associate Professor in the Biomedical Engineering Department, College of Engineering, Sudan University of Sciences and Technology, East Diom, 61 St, P.O. Box 407, Khartoum, Sudan , she and can be reached at: banzier_ibrahim@yahoo.com

Rania .E Mahdi, PhD, is an Assistance Professor in the Biomedical Engineering Department, College of Engineering, Sudan University of Sciences and Technology, East Diom, 61 St, P.O. Box 407, Khartoum, Sudan , she and can be reached at: rania_mahdi@hotmail.com